



Rigidity in Parkinson's disease: evidence from biomechanical and neurophysiological measures

Francesco Asci,^{1,2,†} Marco Falletti,^{1,†} Alessandro Zampogna,¹ Martina Patera,¹
Mark Hallett,³ John Rothwell⁴ and Antonio Suppa^{1,2}

[†]These authors contributed equally to this work.

Although rigidity is a cardinal motor sign in patients with Parkinson's disease (PD), the instrumental measurement of this clinical phenomenon is largely lacking, and its pathophysiological underpinning remains still unclear. Further advances in the field would require innovative methodological approaches able to measure parkinsonian rigidity objectively, discriminate the different biomechanical sources of muscle tone (neural or visco-elastic components), and finally clarify the contribution to 'objective rigidity' exerted by neurophysiological responses, which have previously been associated with this clinical sign (i.e. the long-latency stretch-induced reflex).

Twenty patients with PD (67.3 ± 6.9 years) and 25 age- and sex-matched controls (66.9 ± 7.4 years) were recruited. Rigidity was measured clinically and through a robotic device. Participants underwent robot-assisted wrist extensions at seven different angular velocities randomly applied, when ON therapy. For each value of angular velocity, several biomechanical (i.e. elastic, viscous and neural components) and neurophysiological measures (i.e. short and long-latency reflex and shortening reaction) were synchronously assessed and correlated with the clinical score of rigidity (i.e. Unified Parkinson's Disease Rating Scale—part III, subitems for the upper limb).

The biomechanical investigation allowed us to measure 'objective rigidity' in PD and estimate the neuronal source of this phenomenon. In patients, 'objective rigidity' progressively increased along with the rise of angular velocities during robot-assisted wrist extensions. The neurophysiological examination disclosed increased long-latency reflexes, but not short-latency reflexes nor shortening reaction, in PD compared with control subjects. Long-latency reflexes progressively increased according to angular velocities only in patients with PD. Lastly, specific biomechanical and neurophysiological abnormalities correlated with the clinical score of rigidity.

'Objective rigidity' in PD correlates with velocity-dependent abnormal neuronal activity. The observations overall (i.e. the velocity-dependent feature of biomechanical and neurophysiological measures of objective rigidity) would point to a putative subcortical network responsible for 'objective rigidity' in PD, which requires further investigation.

1 Department of Human Neurosciences, Sapienza University of Rome, 00185 Rome, Italy

2 IRCCS Neuromed Institute, 86077 Pozzilli (IS), Italy

3 Human Motor Control Section, National Institute of Neurological Disorders and Stroke, National Institutes of Health, Bethesda, MD 20814, USA

4 UCL Queen Square Institute of Neurology, London WC1N 3BG, UK

Correspondence to: Antonio Suppa, MD, PhD

Department of Human Neurosciences

Sapienza University of Rome and IRCCS Neuromed Institute

Viale dell'Università 30, 00185, Rome, Italy

E-mail: antonio.suppa@uniroma1.it

Keywords: Parkinson's disease; rigidity; short-latency reflexes; long-latency reflexes; shortening reaction

Introduction

According to the most recent standardized clinical criteria of the International Parkinson and Movement Disorder Society, rigidity is considered a cardinal motor sign in association with bradykinesia for achieving the diagnosis of Parkinson's disease (PD).^{1–3} Parkinsonian rigidity is commonly defined as a uniformly and velocity-independent increased muscle tone probed by the examiner through the passive stretch of muscle groups, which relies on specific articular joints.^{3,4} Parkinsonian rigidity is clinically tested using specific subitems included in the Unified Parkinson's Disease Rating Scale part III (MDS-UPDRS-III),⁵ which are based on subjective semiquantitative measures provided by the examiner.⁶ The clinical assessment of rigidity is also affected by relevant intra- and inter-rater variability limiting the diagnostic accuracy.⁶ Hence, to overcome the intrinsic limitations of a perceptual examination, more objective methodological approaches should be focused on the instrumental evaluation of 'objective rigidity' in PD.

The instrumental investigation of rigidity is also the prerequisite for better understanding the pathophysiological underpinnings of parkinsonian rigidity in PD. Early neurophysiological studies have demonstrated normal short-latency stretch reflexes (SLRs) recorded from forearm flexors following rapid wrist extensions,^{7–10} whereas the long-latency stretch reflexes (LLRs) elicited with similar procedures were increased.^{11–15} However, the specific contribution of abnormal LLRs to limb rigidity, as subjectively perceived by the examiner or objectively assessed by biomechanical measures, has not been thoroughly clarified.^{14,16,17}

Despite being considered a cardinal motor sign in PD, rigidity has been historically the specific focus of a relatively small number of clinical and experimental studies. The limited advances achieved over the last years in the investigation of rigidity in PD would reflect unsolved methodological limitations in the clinical and experimental measurement of this phenomenon.^{18,19} Innovative experimental approaches based on a combined evaluation of biomechanical and neurophysiological measures able to clarify the contribution to 'objective rigidity' exerted by LLRs would gain new insights into the pathophysiology of rigidity in PD.

In this study, we collected biomechanical measures of 'objective rigidity' in patients with PD by using a robotic device able to deliver controlled wrist extensions and estimate specific biomechanical components of rigidity such as those related to neural activity or intrinsic visco-elastic muscular properties.^{20–22} To better discriminate specific biomechanical sources of 'objective rigidity' according to their velocity-dependent features (i.e. viscous and elastic components), we delivered robot-assisted wrist extensions at various angular velocities. To improve the current pathophysiological understanding of parkinsonian rigidity, we also combined the biomechanical measurement of 'objective rigidity' with neurophysiological recordings of stretch-induced muscular responses from wrist flexors (i.e. SLRs and LLRs). Additionally, our neurophysiological evaluation included recordings of long-latency EMG responses from wrist extensors (i.e. shortening reaction—SR) given the putative role of SR previously raised in the pathophysiology of parkinsonian rigidity.²³ Lastly, we correlated all biomechanical and neurophysiological measures of 'objective rigidity' with the standardized clinical evaluation of parkinsonian rigidity.

Materials and methods

Participants

Twenty patients with PD [eight females and 12 males; mean age \pm standard deviation (SD), 67.3 ± 6.9] and a group of 25 age- and sex-matched control subjects (nine females and 16 males; mean age \pm SD, 66.9 ± 7.4) were recruited from the IRCCS Neuromed Institute, Pozzilli (IS), Italy. The experimental study was approved by the Institutional Review Board (NCT05070780) and all participants gave written informed consent. All patients enrolled in the study had a clinical diagnosis of idiopathic PD according to the diagnostic criteria of the International Parkinson and Movement Disorder Society.¹ All participants were right-handed as assessed by the Edinburgh Handedness Scale.²⁴ Baseline demographic and anthropometric parameters, including weight, height, body mass index (BMI), hand size and metacarpal length (distance between the wrist joint and the third metacarpal knuckle) were reported for each participant (Table 1). Participants with pain or manifesting orthopaedic/rheumatological limitations in the upper limbs were excluded. The motor signs and symptoms of PD were assessed utilizing the Hoehn and Yahr (H&Y) scale²⁵ and the MDS-UPDRS-III.⁵ Specifically, to assess the level of rigidity in the most affected upper limb, we used the specific subitem (i.e. subitem 3.3) for rigidity evaluation included in the MDS-UPDRS-III scale (MDS-UPDRS-III-r). Cognitive functions were examined with the Montreal Cognitive Assessment (MoCA)²⁶ and the Frontal Assessment Battery (FAB),²⁷ whereas mood was assessed through the Hamilton Depression Rating Scale (HAM-D).²⁸ Also, only nondemented participants (MoCA \geq 26) were included in the study. None of the participants took any drug acting on the CNS except for dopamine replacement therapy. All patients were evaluated at least 1–2 h after the last intake of the usual dose of L-DOPA and/or other antiparkinsonian drugs and thus in a practically ON state.²⁹ The clinical and anthropometric features of all participants are summarized in Table 1.

Experimental paradigm

The experimental paradigm used in the present study is shown in Fig. 1. Participants sat comfortably on an armchair close to the robotic device designed for the objective assessment of wrist muscle tone (NeuroFlexor, Aggero MedTech AB). Subjects were asked to relax and keep their shoulder in 45° abduction, the elbow in 90° flexion, the forearm in pronation, and the hand placed on the platform of the device during the experiment, following standardized procedures.^{22,30–35} The more affected upper limb was assessed in patients with PD, whereas in control subjects, we investigated the dominant upper limb, in line with the previous studies.^{23,30,36} The robot-assisted device elicited passive hand movements centred on the wrist joint (i.e. wrist extensions), associated with a controlled stretch of the wrist flexors. The robot-assisted wrist extensions were delivered with a specific range of motion (ROM) of 50° (i.e. ranging from -20° to $+30^\circ$) following standardized procedures.³⁷ Concerning the angular velocity, the robot-assisted wrist extensions were administered at seven different angular velocities randomly applied (i.e. 5–50–100–150–200–236–280°/s). The robot-assisted device reaches the target angular velocity with an angular

Table 1 Demographic, anthropometric and clinical features of participants

	Age (years)	Gender n (%)		Weight (kg)	Height (cm)	BMI (kg/m ²)	Metacarpal length (mm)	Hand mass (kg)	MoCA	FAB	HAM-D	Disease duration (year)	H&Y	MDS-UPDRS-III	MDS-UPDRS-III-r
		M	F												
PD	67.3 ± 6.9	12 (60)	8 (40)	74.0 ± 14.2	168.5 ± 9.5	25.9 ± 3.5	97.0 ± 9.8	0.4 ± 0.1	27.4 ± 1.2	16.5 ± 1.3	2.1 ± 1.6	5.1 ± 2.5	2.1 ± 0.6	21.8 ± 8.2	2.1 ± 0.8
HS	66.9 ± 7.4	16 (64)	9 (36)	73.1 ± 13.7	173.1 ± 9.7	24.3 ± 3.5	92.0 ± 13.2	0.4 ± 0.1	27.7 ± 1.4	17.0 ± 1.0	1.8 ± 1.4	–	–	–	–

BMI = body mass index; FAB = Frontal Assessment Battery; HAM-D = Hamilton Depression Scale; HS = healthy subjects; H&Y = Hoehn and Yahr scale; MoCA = Montreal Cognitive Assessment; MDS-UPDRS-III = Unified Parkinson's Disease Rating Scale part III; MDS-UPDRS-III-r = subitem for right upper limb rigidity; PD = Parkinson's disease.

acceleration of ~13°/s².³¹ The experimental paradigm consisted of six independent sessions each based on the acquisition of five trials at slow angular velocity (5°/s) (basal measurements) and 10 trials at one of the six remaining angular velocities randomly delivered, with an inter-trial interval of at least 10 s, and inter-session interval of 5 min. Accordingly, the whole experiment consisted of 90 wrist extensions in total (i.e. 30 slow angular velocity trials + 60 fast angular velocity trials). The specific range of angular velocities was selected to examine velocity-dependent biomechanical changes in control subjects and patients with PD. For this purpose, a slow angular velocity of 5°/s was included as a reference for the system since it is below the threshold for spindle activation in distal muscle.³⁸ Moreover, we selected angular velocities ranging from 50°/s to 280°/s since angular velocities below 70°/s,³⁹ and above 300°/s provide no additional information.¹⁴ Conversely, angular velocities ranging from 140 to 190°/s are the most sensitive to muscle tone detection.³⁹ Also, the angular velocity of 236°/s was selected to conform with the previous procedures.³¹ Lastly, the calibration of the robot-assisted device required five additional trials for each value of angular velocity, implying robotic movements given alone (i.e. without the arm of a participant)³¹ (Fig. 2A and B).

Biomechanical measures

The biomechanical measures were acquired and analysed using a dedicated algorithm included in the robotic device designed for the objective assessment of wrist muscle tone. In more detail, during the fast run, three specific points of force are identified: a first point (P0) at the beginning of the fast robotic movement and two further points (P1 and P2) during fast robotic movements. Moreover, a final point of force (P3) is calculated 1 s after the end of slow robotic movements. After collecting several trials of fast and slow robotic movements, the algorithm interpolates the four points of force (P0, P1, P2 and P3), using a standard setting. Then, the algorithm estimates passive (inertia, resting tension, elasticity and viscosity) and active (neural) biomechanical components of muscle tone. Among the estimated passive biomechanical components, the inertial component (IC) represents the main resistance to the hand and platform acceleration. IC is calculated from the following formula:

$$IC = m \times a \tag{1}$$

where *m* is the sum of hand and movable platform masses and *a* represents the angular acceleration. Conventionally, the hand mass is approximated at 0.6% of body weight. Hence, IC is calculated for each participant being a constant value throughout the experiment. Moreover, the resting tension is estimated by using the point of force P0 extracted from the total resisting force which reflects the hand mass before the stretch onset. As for IC, resting tension can be also considered a constant value for each participant during the experiments. Concerning the elastic component (EC), the biomechanical model considers it as a length-dependent resisting force that increases the more the muscles and tendons are stretched and includes both the linear elasticity and the non-linear end range stiffness. Accordingly, EC is estimated by using the point of force P3 recorded 1 s after the end of the slow robotic movement. By contrast, the viscous component (VC) is a velocity-dependent resisting force made up of an early component that is high during the initial acceleration and a late component that is maintained during the remaining muscle stretch. The early component of VC is estimated at the point of force P1 by subtracting IC from the total resisting force.

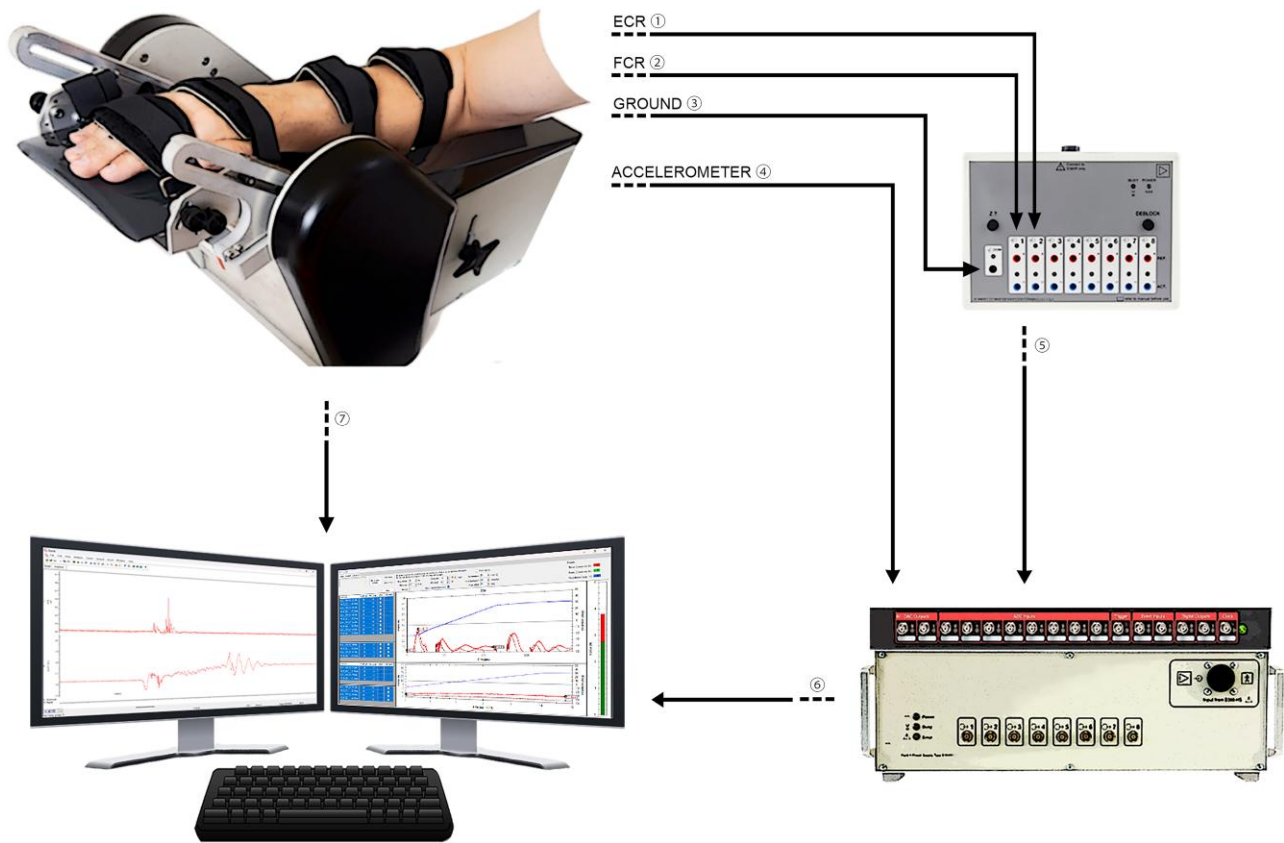


Figure 1 Experimental paradigm. Top left: Robotic device used for delivering controlled wrist extensions at various angular velocities and allowing the objective assessment of muscle tone. Top right: EMG signal recorded from the extensor carpi radialis (ECR) (line 1) and flexor carpi radialis (FCR) (line 2) using a couple of surface electrodes and a ground (line 3). Bottom right: Synchronization and digitalization by using A/D laboratory interface of raw signals recorded by a triaxial accelerometer (line 4) and surface EMG electrodes (line 5). Bottom left: The workstation used for online inspection and offline analysis of synchronized neurophysiological (line 6) and biomechanical measures (line 7).

Differently, the late component of VC is conventionally approximated as 20% of the early viscosity, based on previous reports.⁴⁰ Furthermore, the neural component (NC) is estimated at the point of force P2, corresponding to the maximal extension at the end of the fast robotic movement by subtracting EC and VC components from the total resisting force. The estimated biomechanical components are corrected for age, weight and metacarpal length, using a standard setting and finally displayed by a graphic interface.^{30,31} Lastly, the algorithm calculates the total force (TF) by adding the five estimated biomechanical components of muscle tone (inertial, resting tension, EC, VC and NC) through the following mathematical equation also described in previous methodological studies:

$$TF(q) = EC(q) + VC(q) + NC(q) \quad (2)$$

where TF is the total force, EC is the elastic force, VC is the viscous force and NC is the neural force and q indicates a specific angle.^{30,31,41} IC and resting tension are not included in Equation (2) since both are constant values already included in the estimation of VC, EC and NC.

Neurophysiological measures

EMG was recorded from the flexor and extensor carpi radialis muscles [flexor carpi radialis (FCR) and extensor carpi radialis (ECR)], through surface electrodes according to standardized procedures.⁴²

The raw EMG signal was sampled at 5 kHz with a CED 1401 A/D laboratory interface (Cambridge Electronic Design), amplified and filtered (20 Hz–2 kHz bandwidth) with a Digitimer D360 (Digitimer Ltd). The data were online visually inspected and stored on a workstation for offline analysis (Signal Software, Cambridge Electronic Design, Cambridge, UK). We analysed EMG in a time window starting at 100 ms before the robot-assisted wrist extensions to 100 ms after the end of the robotic displacement (see Figs 1 and 2C–H for further details). To exclude the possible influence on SLRs, LLRs and SRs of background muscle activity occurring in the 100 ms preceding robot-assisted wrist extensions, we excluded trials showing EMG activity $>50 \mu\text{V}$ from further analysis. We then rectified all EMG signals and averaged 10 trials collected for each trial. The SLRs, LLRs and SRs were all calculated according to standardized procedures i.e. vertical cursors were first placed according to the expected latency of EMG responses (i.e. 25–45 ms for SLRs, 50–100 ms for LLRs and finally 120 ± 15 ms for SRs)^{23,36} and cursor position was then visually optimized to restrict the analysis to EMG bursts of at least $50 \mu\text{V}$ ^{14,43,44} (Fig. 2C–H). Also, besides short and long-reflexes, we verified possible additional stretch-induced EMG activity by measuring the area under the curve (AUC) of EMG activity recorded from the onset of SLR to the end of the robot-assisted wrist displacement. The simultaneous recordings of EMG and biomechanical measures during the robot-assisted wrist extensions were allowed by a dedicated script *ad hoc* designed to receive input signals from a triaxial accelerometer (E.M.S. s.r.l) placed at the level of the III metacarpus (Fig. 1).

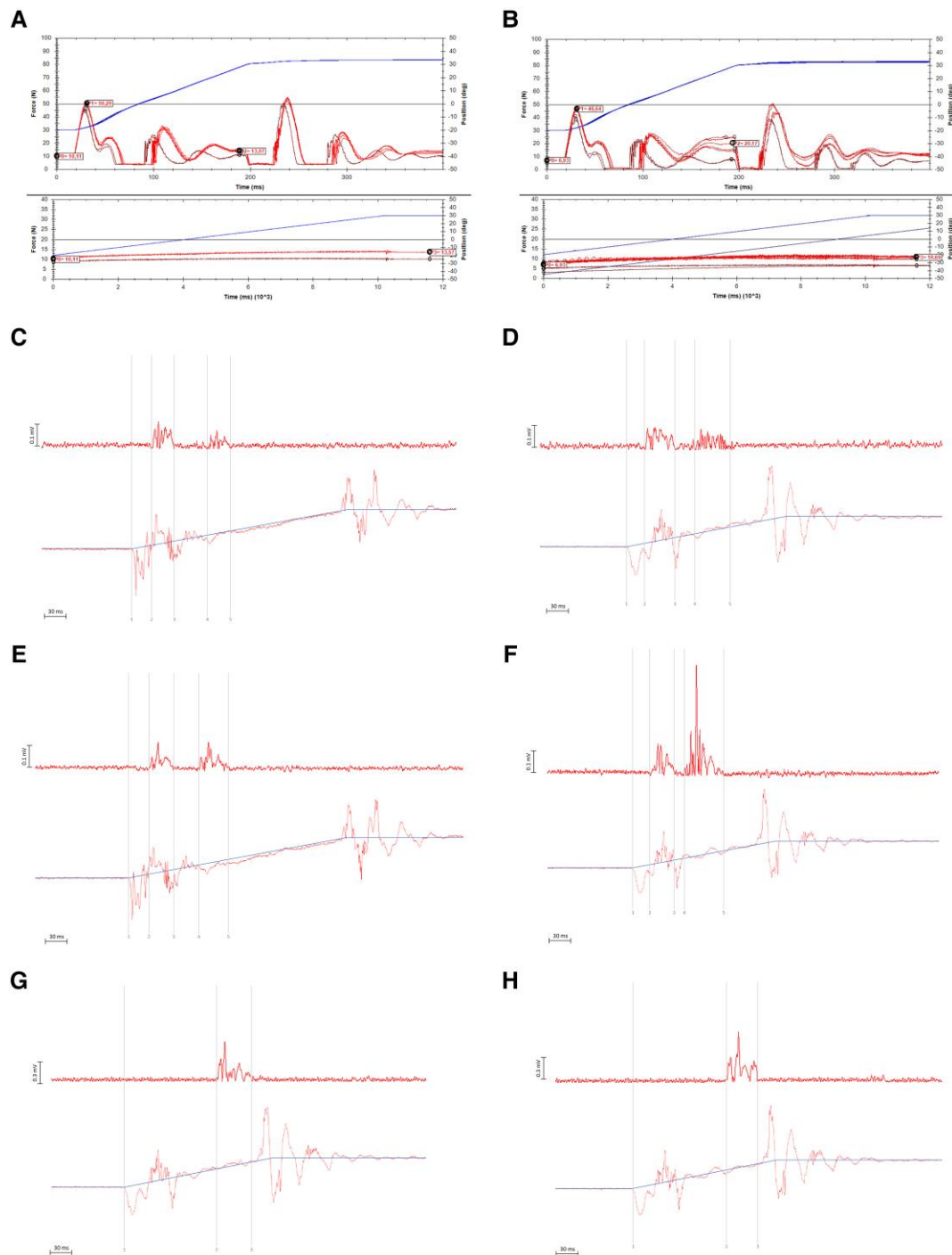


Figure 2 Experimental design. (A and B) Example of biomechanical measurements during robotic-assisted wrist extensions, in a representative healthy subject (HS) (A) and PD patient (B). The blue line represents the robotic displacement in degrees (-20° to $+30^{\circ}$). Dark red lines indicate the total force (TF) recorded during the robotic device displacement alone (i.e. under calibration). Red lines indicate the TF recorded during the robotic device displacement (the upper panel shows fast displacements at $280^{\circ}/s$; the lower panel shows slow displacements at $5^{\circ}/s$). The figure also shows four 'points of force' (P0, P1, P2 and P3), which are interpolated to calculate the passive (viscosity and elasticity) and active components (neural) of the 'objective rigidity', using a dedicated algorithm (see 'Materials and methods' section). (C–F) Example of rectified EMG activity recorded from the flexor carpi radialis (FCR) muscle (red line above) and accelerometric signal (red line below) recorded during the robot-assisted wrist extension at slow ($100^{\circ}/s$) (C–E) and fast ($280^{\circ}/s$) (D–F) angular velocity, in a representative healthy subject (C and D) and PD patient (E and F). The blue line represents the robotic displacement in degrees (-20° to $+30^{\circ}$). In all panels, the vertical cursors indicate how neurophysiological responses [i.e. short-latency reflexes (SLRs) and long-latency reflexes (LLRs)] have been identified and measured. 1 \leftrightarrow 2: SLR latency; 2 \leftrightarrow 3: SLR duration, amplitude and area under the curve (AUC); 1 \leftrightarrow 4: LLR latency; 4 \leftrightarrow 5: LLR duration, amplitude and AUC, according to standardized procedures. Note that although SLRs were comparable in the healthy subject and PD patient at all angular velocities, the amplitude and AUC of LLRs were higher in the PD patient than in the healthy subject at an angular velocity of $280^{\circ}/s$. (G and H) Example of rectified EMG activity recorded from the extensor carpi radialis (ECR) muscle (red line above) and accelerometric signal (red line below) recorded during the robot-assisted wrist extension $280^{\circ}/s$ in a representative healthy subject (G) and PD patient (H). The vertical cursors indicate how neurophysiological responses [i.e. shortening reactions (SRs)] have been identified and measured. 1 \leftrightarrow 2: SR latency; 2 \leftrightarrow 3: SR duration, amplitude and AUC.

Statistical analysis

We did not determine the sample size of participants *a priori*, because of the exploratory nature of the present study, which is based on an innovative experimental design never used before and employing combined clinical, biomechanical and neurophysiological recordings. Therefore, we used a standard frequentist method based on sequential analysis. The normality of all variables was assessed using the Kolmogorov-Smirnov test. The χ^2 test was used to compare gender distribution in controls and patients. The Student's unpaired t-test was used to compare demographic (i.e. age) and anthropometric parameters and clinical scales (i.e. MoCA, FAB and BMI), in controls and patients. The Student's unpaired t-test was also used to compare EMG amplitudes and AUC before and after robot-assisted wrist displacement in both groups. A mixed-ANOVA design was used to compare the possible variations of all biomechanical (i.e. EC, VC, NC and TF) and neurophysiological (i.e. latency, duration, area and AUC of the SLRs, LLRs and SRs) measures as a function of the various angular velocities by using 'velocity' (six levels: 50–100–150–200–236–280°/s) as a within-group factor and 'group' (controls and PD) as the between-group factor of analysis. All recorded biomechanical and neurophysiological data were considered in the mixed-ANOVA analysis, including null data. In case of violations of sphericity at the Mauchly's test on the factor 'velocity', the Greenhouse-Geisser corrections were applied. Tukey's honest significance test was used for *post hoc* analysis. We used the Spearman's rank test for assessing possible correlations between relevant clinical, biomechanical and neurophysiological measures. Given the standard frequentist method here applied for statistics, the level of significance initially set at $P < 0.05$ was corrected, according to the Pocock's procedure for sequential analysis to $P = 0.0184$ (approximated to 0.02), considering four interim analysis.^{45–47} Values are presented as mean \pm SD. Statistical analyses were performed using STATISTICA version 10.0 (TIBCO Software Inc.).

Data availability

All clinical and instrumental data are stored offline at the IRCCS Neuromed Institute and the Department of Human Neurosciences, Sapienza University of Rome, Italy and are available on reasonable request to the corresponding author.

Results

Demographic and anthropometric variables were normally distributed in controls and patients and were all comparable in the two groups: age ($t = 0.17$; $P = 0.87$), weight ($t = 0.20$; $P = 0.84$), height ($t = -1.61$; $P = 0.11$), BMI ($t = 1.54$; $P = 0.13$), hand weight ($t = 0.20$; $P = 0.84$) and metacarpal length ($t = 1.39$; $P = 0.17$). Also, the MoCA ($t = -0.72$; $P = 0.48$), FAB ($t = -1.47$; $P = 0.15$) and HAM-D ($t = 0.56$; $P = 0.58$) scores were comparable between controls and patients with PD (Table 1). All the collected experimental data were included in the analysis and no 'outliers' were excluded. The detailed output of the statistical analysis, including all Greenhouse-Geisser corrections, is reported in Supplementary material 1.

Biomechanical measures

The total force (TF) differed between controls and PD patients, as shown by the significant effect of the factor 'velocity' [$F_{(5,215)} = 36.99$, $P < 0.01$], 'group' [$F_{(1,43)} = 60.33$, $P < 0.01$] and the

'velocity' \times 'group' interaction [$F_{(5,215)} = 24.56$, $P < 0.01$]. The *post hoc* analysis revealed a significant effect of factor 'velocity' in PD [$F_{(5,95)} = 29.88$, $P < 0.01$] and controls [$F_{(5,120)} = 3.34$, $P < 0.01$]. In PD patients, TF significantly increased at 200°/s ($P < 0.01$), 236°/s ($P < 0.01$), and finally 280°/s ($P < 0.01$), whereas in healthy subjects, it did not. Although TF was comparable in controls and patients at 50°/s ($P = 0.99$), it differed in the two groups being significantly greater in PD patients than in controls at angular velocities of 150°/s ($P = 0.02$), 200°/s ($P < 0.01$), 236°/s ($P < 0.01$), and finally 280°/s ($P < 0.01$) (Fig. 3A and Table 2).

Concerning elasticity (EC), ANOVA showed comparable values in controls and patients for all angular velocities as shown by the non-significant factor 'velocity' [$F_{(5,215)} = 1.60$, $P = 0.16$] and 'group' [$F_{(1,43)} = 2.45$, $P = 0.13$] (Fig. 3B and Table 2).

The viscosity (VC) increased significantly with angular velocities and did so to a similar extent in controls and PD patients, as shown by the significant effect of the factor 'velocity' [$F_{(5,215)} = 22.56$, $P < 0.01$] and the non-significant effect of the factor 'group' [$F_{(1,43)} = 0.12$, $P = 0.73$], and the 'velocity' \times 'group' interaction [$F_{(5,215)} = 0.67$, $P = 0.65$]. Viscosity increased significantly in PD patients [$F_{(5,95)} = 18.23$, $P < 0.01$] and similarly in controls [$F_{(5,120)} = 10.93$, $P < 0.01$] starting in from 100°/s (all $P < 0.02$) in PD patients and from 150°/s (all $P < 0.02$) in healthy subjects. Viscosity was comparable in controls and patients at all values of angular velocities (Fig. 3C and Table 2).

The neural component (NC) differed between controls and PD patients, as shown by the significant effect of the factor 'velocity' [$F_{(5,215)} = 38.14$, $P < 0.01$] and 'group' [$F_{(1,43)} = 146.32$, $P < 0.01$], and the 'velocity' \times 'group' interaction [$F_{(5,215)} = 43.04$, $P < 0.01$]. There was a significant effect of factor 'velocity' in PD [$F_{(5,95)} = 37.13$, $P < 0.01$] but not in controls [$F_{(5,120)} = 0.55$, $P = 0.74$]. In PD patients, NC increased significantly at angular velocities of 200°/s ($P < 0.01$), 236°/s ($P < 0.01$) and 280°/s ($P < 0.01$), whereas in healthy subjects it did not. NC was comparable in controls and patients at 50–100 and 150°/s, whereas it progressively increased being higher in patients than in controls at angular velocities of 200°/s ($P < 0.01$), 236°/s ($P < 0.01$) and 280°/s ($P < 0.01$) (Fig. 3D and Table 2).

Neurophysiological measures

Student's t-test for independent measures showed comparable background muscle activity occurring before as well as after robot-assisted wrist displacement in the two groups, in all experiments.

We failed to record neurophysiological responses in controls and patients during robot-assisted wrist extensions at angular velocities of 5°/s and 50°/s. Conversely, angular velocities ≥ 100 °/s increased the likelihood of recording two independent bursts of EMG activity from the FCR at latencies of about 30 ms (i.e. SLR) and 80 ms (i.e. LLR). Lastly, angular velocities ≥ 100 °/s also increased the likelihood of recording a single burst of EMG from the ECR at latencies of about 120 ms (i.e. SR).

Short-latency stretch reflexes

We obtained reliable SLRs at 100°/s in 32% (8/25) of controls and 35% (7/20) of PD patients, at 150°/s in 56% (14/25) of controls and 55% (11/20) of PD patients, at 200°/s in 72% (18/25) of controls and 70% (14/20) of PD patients, at 236°/s in 80% (20/25) of controls and 80% (16/20) of PD patients and, finally at 280°/s in 80% (20/25) of controls and 85% (17/20) of PD patients. The χ^2 test showed a comparable distribution of SLR frequencies in controls and patients with PD.

Between-group ANOVAs included neurophysiological data recorded in all participants, regardless of the presence of a

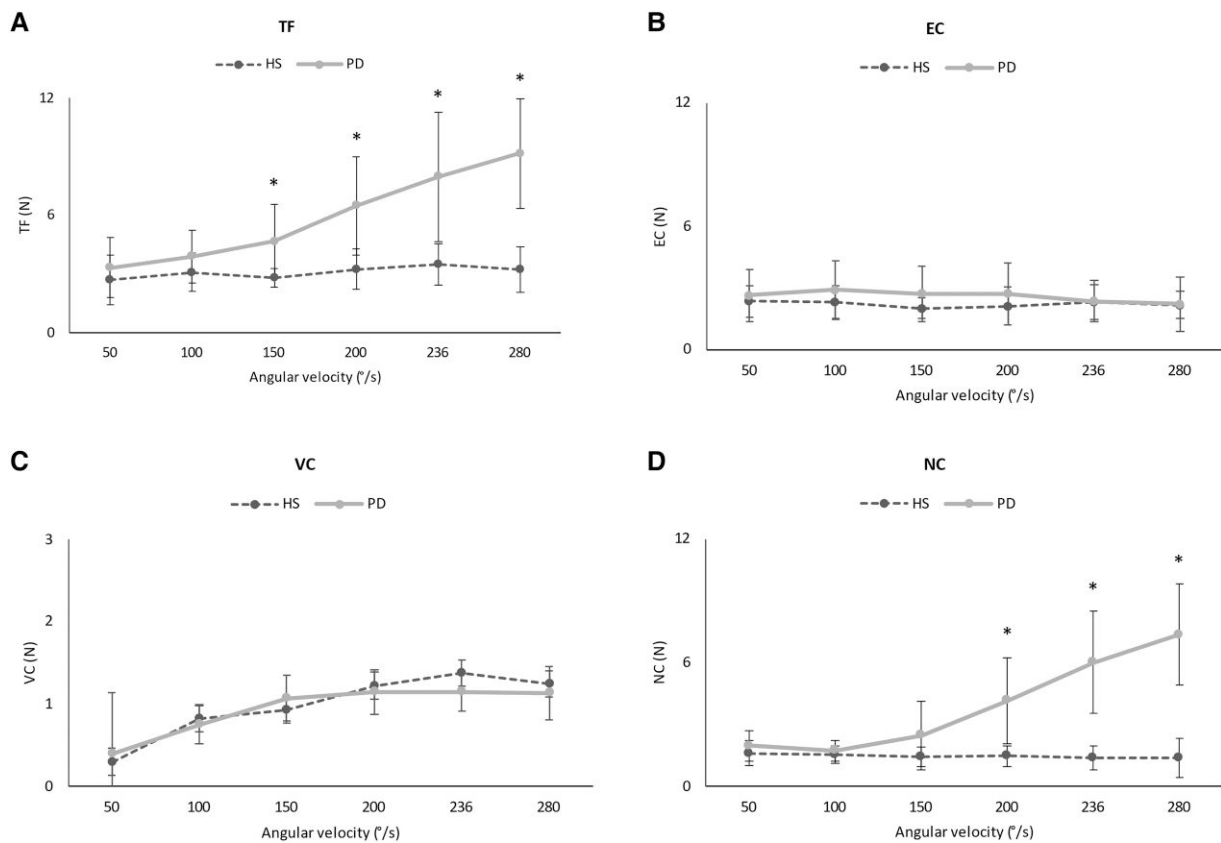


Figure 3 Biomechanical measures. Biomechanical measures achieved during robot-assisted wrist extensions delivered at different angular velocities, in healthy subjects (HS, dashed lines) and patients with Parkinson's disease (PD, continuous lines) (A) Total force (TF). (B) Elastic component (EC). (C) Viscous component (VC). (D) Neural component (NC). * $P < 0.05$.

measurable SLRs at each angular velocity, and thus including null data. Angular velocity did not modify SLRs in controls and patients, as indicated by the non-significant effect of the factor 'velocity' [latency: $F_{(4,36)} = 2.48$, $P = 0.06$; duration: $F_{(4,48)} = 0.76$, $P = 0.55$; amplitude: $F_{(4,40)} = 1.15$, $P = 0.35$; and AUC: $F_{(4,120)} = 0.54$, $P = 0.64$], and 'group' in all comparisons [latency: $F_{(1,9)} = 1.11$, $P = 0.32$; duration: $F_{(1,12)} = 0.24$, $P = 0.63$; amplitude: $F_{(1,10)} = 0.10$, $P = 0.34$; and AUC: $F_{(1,30)} = 0.21$, $P = 0.65$] (Fig. 4A–D and Table 2).

Long-latency stretch reflexes

We obtained reliable LLRs at 100°/s in 12% (3/25) of controls and 45% (9/20) of PD patients, at 150°/s in 20% (5/25) of controls and 70% (14/20) of PD patients, at 200°/s in 32% (8/25) of controls and 70% (17/20) of PD patients, at 236°/s in 52% (13/25) of controls and 95% (19/20) of PD patients, and finally at 280°/s in 48% (12/25) of controls and 95% (19/20) of PD patients. The χ^2 test showed that LLRs frequency was higher in PD patients than controls at angular velocities of 150°/s ($P < 0.01$), 200°/s ($P < 0.01$), 236°/s ($P < 0.01$) and 280°/s ($P < 0.01$), whereas at 100°/s it did not.

Between-group ANOVAs included neurophysiological data recorded in all participants, regardless of the presence of a measurable LLRs at each angular velocity, and thus including null data. Angular velocity did not modify the latency and duration of LLRs in controls and PD patients, as indicated by the non-significant effect of the factor 'velocity' [latency: $F_{(4,40)} = 2.46$, $P = 0.06$; duration: $F_{(4,40)} = 1.02$, $P = 0.41$] and 'group' in all comparisons [latency: $F_{(1,10)} = 0.001$, $P = 0.98$; duration: $F_{(1,10)} = 2.99$, $P = 0.11$] (Fig. 5A and B and Table 2). Conversely, concerning amplitudes, between-group

ANOVA showed the significant effect of the factor 'group' [$F_{(1,10)} = 65.15$, $P < 0.01$] and a borderline significant effect of the factor 'velocity' [$F_{(4,40)} = 4.27$, $P = 0.0197$] and 'velocity' × 'group' interaction [$F_{(4,40)} = 4.34$, $P = 0.0186$]. There was a significant effect of factor 'velocity' in PD patients [$F_{(4,32)} = 13.72$, $P < 0.01$] but not in controls [$F_{(4,8)} = 3.00$, $P = 0.09$]. Differently from healthy subjects, in PD, LLRs amplitude increased significantly at 150°/s ($P < 0.01$), 200°/s ($P < 0.01$), 236°/s ($P < 0.01$) and finally 280°/s ($P < 0.01$). Although similar LLRs amplitudes were found in controls and patients at 100°/s ($P = 0.97$), the amplitudes progressively increased being higher in PD than in controls at angular velocities of 150°/s ($P < 0.01$), 200°/s ($P < 0.01$), 236°/s ($P < 0.01$) and finally 280°/s ($P < 0.01$) (Fig. 5C and Table 2). Furthermore, concerning LLRs AUC, between-group ANOVA showed a significant effect of the factor 'velocity' [$F_{(4,42)} = 6.78$, $P < 0.01$], 'group' [$F_{(1,8)} = 50.58$, $P < 0.01$] and the 'velocity' × 'group' interaction [$F_{(4,32)} = 5.51$, $P < 0.01$]. There was a significant effect of factor 'velocity' in patients [$F_{(4,24)} = 15.96$, $P < 0.01$] but not in controls [$F_{(4,8)} = 0.66$, $P = 0.64$]. In PD patients, the AUCs increased significantly at 236°/s ($P = 0.019$) and 280°/s ($P < 0.01$). Although AUCs were similar in controls and patients at 100–150 and 200°/s, AUCs progressively increased being higher in PD than in controls at angular velocities of 236°/s ($P < 0.01$) and 280°/s ($P < 0.01$) (Fig. 5D and Table 2).

Shortening reaction

We obtained reliable SRs at 100°/s in 8% (2/25) of controls and 25% (5/20) of PD patients, at 150°/s in 12% (3/25) of controls and 35% (7/20) of PD patients, at 200°/s in 20% (5/25) of controls and 35% (7/20) of PD patients, at 200°/s in 20% (5/25) of controls and 35% (7/20)

Table 2 Biomechanical and neurophysiological measures of participants

	Biomechanical measures				Neurophysiological measures											
	TF (N)	EC (N)	VC (N)	NC (N)	SLRs			LLRs			SRS			AMP (mV)	AUC (μ Vs)	
					LAT (ms)	DUR (ms)	AMP (mV)	AUC (μ Vs)	LAT (ms)	DUR (ms)	AMP (mV)	AUC (μ Vs)	LAT (ms)	DUR (ms)	AMP (mV)	AUC (μ Vs)
PD	9.16 ± 3.11	2.23 ± 1.33	-0.40 ± 0.32	7.35 ± 2.46	32.9 ± 4.9	36.5 ± 11.5	0.20 ± 0.17	2.2 ± 2.3	80.7 ± 10.7	51.4 ± 10.7	0.42 ± 0.16	8.4 ± 2.3	125 ± 7.9	48 ± 14	0.31 ± 0.2	5.0 ± 1.2
HS	3.24 ± 1.16	2.19 ± 0.68	-0.34 ± 0.40	1.39 ± 0.95	32 ± 3.1	37 ± 8.7	0.19 ± 0.11	2.4 ± 1.6	78 ± 12	41 ± 12	0.16 ± 0.1	1.3 ± 0.3	103 ± 25	68 ± 22	0.33 ± 0.2	5.9 ± 1.2

Biomechanical and neurophysiological measures collected in patients with Parkinson's disease (PD) and healthy subjects (HS) during robot-assisted wrist extensions delivered at an angular velocity of 280°/s. AMP = amplitude; AUC = area under the curve; DUR = duration; EC = elastic component; LAT = latency; LLRs = long-latency reflexes; NC = neural component; LAT = latency; LLRs = long-latency reflexes; SRS = shortening reaction; TF = total force; VC = viscous component.

of PD patients, at 236°/s in 28% (7/25) of controls and 40% (8/20) of PD patients and, finally at 280°/s in 36% (9/25) of controls and 55% (11/20) of PD patients. The χ^2 test showed a comparable distribution of SR frequencies in control subjects and PD patients.

Angular velocity did not modify SRs in controls and in PD patients, as indicated by the non-significant effect of the factor 'velocity' [latency: $F_{(4,20)} = 0.28$, $P = 0.89$; duration: $F_{(4,20)} = 0.77$, $P = 0.56$; amplitude: $F_{(4,20)} = 1.54$, $P = 0.23$; and AUC: $F_{(4,20)} = 2.68$, $P = 0.06$] and 'group' for all comparisons [latency: $F_{(1,5)} = 2.87$, $P = 0.15$; duration: $F_{(1,5)} = 1.11$, $P = 0.34$; amplitude: $F_{(1,5)} = 0.01$, $P = 0.92$; and AUC: $F_{(1,5)} = 0.09$, $P = 0.78$] (Table 2 and Supplementary material 2).

Correlations

We used the Spearman test to assess correlation between a specific subset of relevant clinical (MDS-UPDRS-III-r), biomechanical (TF and NC) and neurophysiological (LLRs and SLR AMP) measures collected at the angular velocity of 280°/s. Hence, after correction for multiple comparisons (adjusted $P = 0.02/6$), the level of significance of our correlation analysis was set at $P < 0.003$. The clinical measure of rigidity (MDS-UPDRS-III-r) correlated with the biomechanical assessment of 'objective rigidity' (i.e. TF) ($r = 0.61$; $P = 0.004$) and with the estimated neuronal component (NC) ($r = 0.58$, $P = 0.008$), even though both correlations did not survive correction for multiple comparisons (Fig. 6A and B). TF correlated significantly with NC ($r = 0.86$, $P < 0.01$) (Fig. 6C). Also, the amplitude of LLRs showed a correlation with TF ($r = 0.57$, $P = 0.01$), that did not survive correction for multiple comparisons (Fig. 6D), and a significant correlation with the NC ($r = 0.69$, $P < 0.01$) (Fig. 6E). Lastly, there was no correlation between SLR and LLRs ($r = 0.28$, $P = 0.32$) (Fig. 6F).

Discussion

Our experimental design implying robot-assisted wrist extensions allowed us to measure 'objective rigidity' in PD and clarify the velocity-dependent feature of specific biomechanical and neurophysiological abnormalities responsible for this phenomenon. Our experimental observations provide advances in the current understanding of the pathophysiology of rigidity in PD.

Biomechanical measures of rigidity

Differently from controls, patients manifested an enhancement of total force (TF), and in turn 'objective rigidity', with a progressive increase of angular velocities (i.e. the faster angular velocity, the greater TF and thus objective rigidity). Our findings support previous evidence of a velocity-dependent feature of parkinsonian rigidity^{48–51} and are fully in agreement with the single previous observation in PD using the same robot-assisted device.²² Moreover, the main biomechanical component of 'objective rigidity' in PD arose from neural activity rather than reflecting intrinsic visco-elastic components.^{22,39,51} Furthermore, the amount of neural activity estimated by the algorithm (i.e. NC) strongly correlated with 'objective rigidity' (i.e. TF), and both values showed a correlation trend with MDS-UPDRS-III rigidity subitems (i.e. the greater TF and NC, the higher the clinical severity of rigidity).²² Although, as expected, the estimated viscous component progressively increased with angular velocities, it did so comparably in controls and patients with PD thus excluding a significant contribution of viscous components to 'objective rigidity' in PD.^{22,39,51} Taken together, our robot-assisted methodology allowed us to measure 'objective rigidity' in PD, report its velocity-dependent features, and

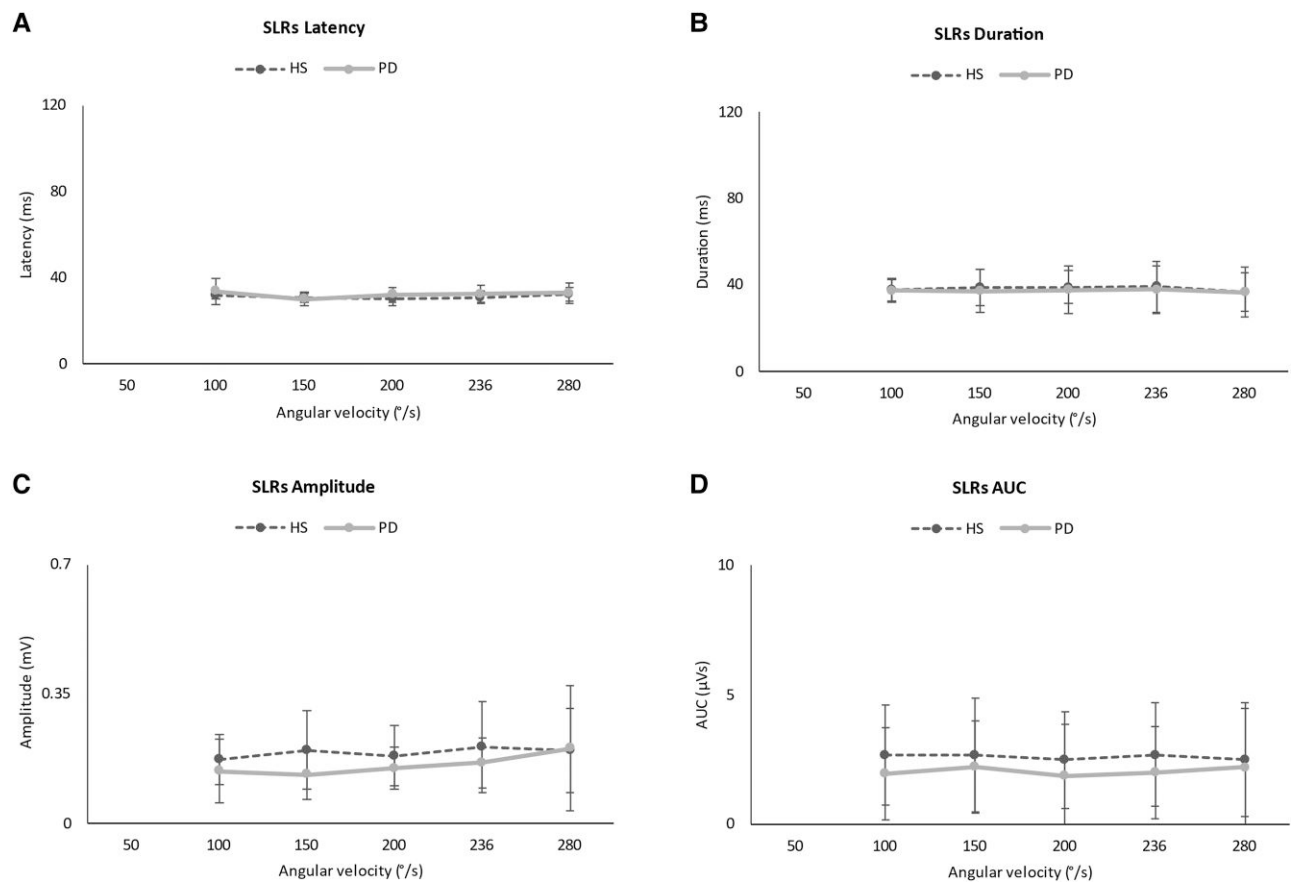


Figure 4 Short-latency reflexes (SLRs). SLRs measured during robot-assisted wrist extensions delivered at different angular velocities, in healthy subjects (HS) (dashed lines) and patients with Parkinson's disease (PD) (continuous lines). (A) Latency. (B) Duration. (C) Amplitude. (D) Area under the curve (AUC). Note that SLRs were unrecordable in HS and PD patients at an angular velocity of 50°/s.

support neuronal activity as the main source of this biomechanical phenomenon.

Neurophysiological measures of rigidity

By demonstrating comparable SLRs in controls and patients, under all angular velocities, our neurophysiological investigation confirmed that 'objective rigidity' in PD does not reflect increased excitability of spinal circuits generating short-latency responses.^{8–10,52} We, therefore, confirm that SLRs do not contribute to 'objective rigidity' in PD.

Here we provide the first evidence of a velocity-dependent feature of LLRs in PD. In addition to the well known increase in amplitude and AUC of LLRs in PD,^{14,15,52,53} we report here a progressive increase in LLRs along with the rise of angular velocity. Still, we found a strong correlation between LLRs amplitude and the estimation of the biomechanical neural component of 'objective rigidity' (i.e. the higher amplitude of LLRs, the greater NC). In summary, we demonstrated that the velocity-dependent changes in LLRs parallel those observed during the biomechanical measurement of 'objective rigidity' in PD.⁵¹

The specific pathophysiological contribution of increased LLRs to 'objective rigidity' in PD is difficult to argue.^{36,44} The hypothesis that 'objective rigidity' in PD is simply caused by increased amplitudes of LLRs can be easily discarded since LLRs consist of EMG responses characterized by low amplitude and short duration, which are not compatible with the overall clinical and biomechanical evaluation of rigidity. Our experimental design implied phasic

rather than tonic robot-assisted wrist extensions. Hence, it is reasonable that a prolonged muscle stretch would have more likely elicited sustained or tonic EMG activity after LLRs thus explaining what is clinically perceived as 'lead pipe' rigidity. The concurrent velocity-dependent changes of (enhanced) LLRs and biomechanical measures of 'objective rigidity' would suggest, however, that LLRs reflect the activation of neuronal loops at least partly overlapping with those contributing to rigidity in PD. Hence, LLRs could be considered a neurophysiological measure probing neuronal pathways associated with rigidity in PD. Further supporting the contribution of LLRs to the pathophysiology of rigidity in PD, we found that both LLRs and 'objective rigidity' (i.e. total force and estimation of the neural component) increased progressively, starting from angular velocities of 150°/s, confirming the previous reports.³⁹ Given that the typical clinical manoeuvres for muscle tone assessment imply angular velocities ranging from 60 to 200°/s,^{13,54} our findings would also suggest that faster wrist displacements more likely allow a clear detection of rigidity in patients with PD.

Lastly, we excluded a relevant contribution to 'objective rigidity' exerted by shortening reactions (SRs). The SR consists of a long-latency stretch-induced EMG response recorded from the antagonist muscle and still of unknown origin.⁵⁵ Our observations are not in line with previous studies demonstrating a significant relationship in PD between the SRs and the torque-angle slope, likely due to different methodologies used.^{23,51,56} Overall, our findings suggest that the excitability of neuronal circuits generating shortening reactions^{50,51} operated within normal ranges in PD.

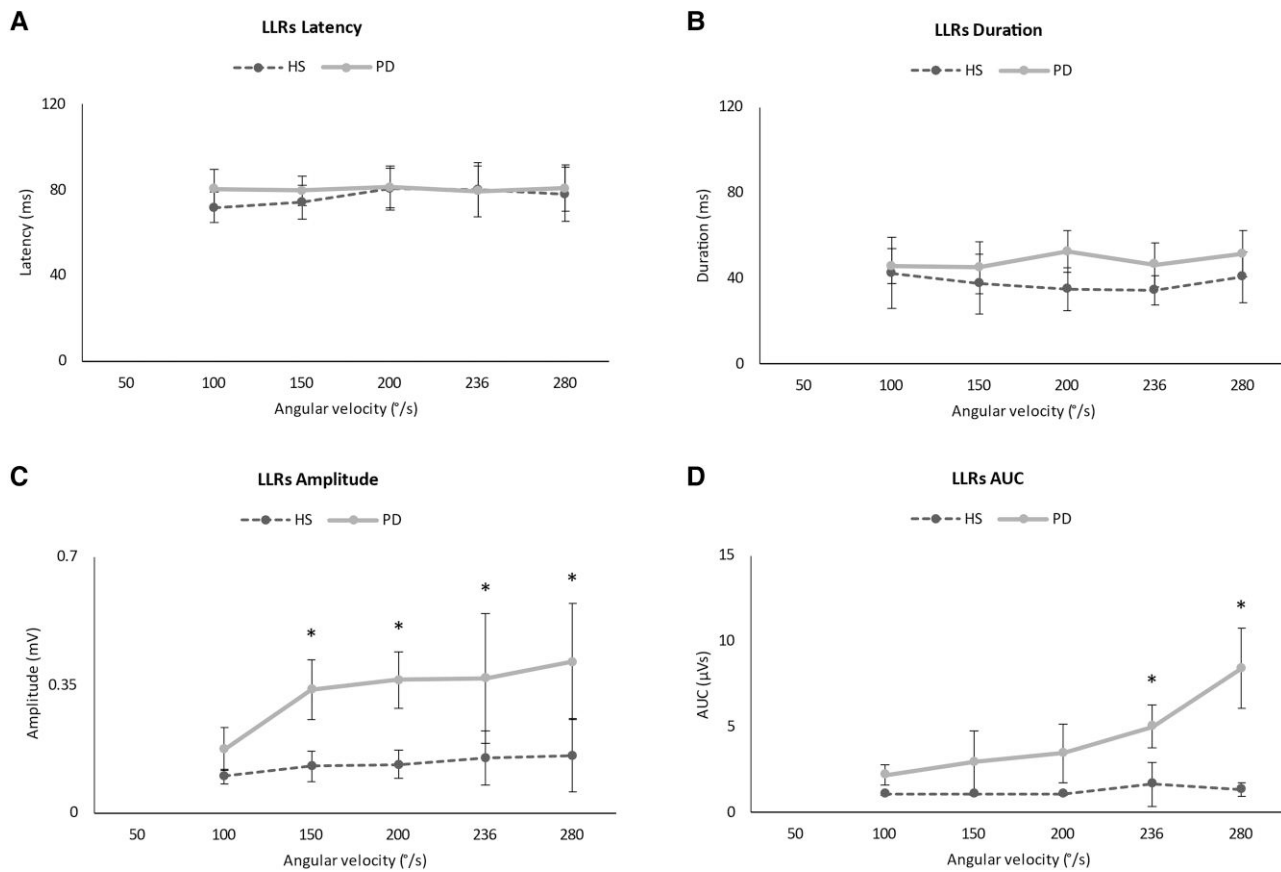


Figure 5 Long-latency reflexes (LLRs). LLRs measured during robot-assisted wrist extensions delivered at different angular velocities, in healthy subjects (HS) (dashed lines) and patients with Parkinson's disease (PD) (continuous lines). (A) Latency. (B) Duration. (C) Amplitude. (D) Area under the curve (AUC). Note that LLRs were unrecordable in HS and PD patients at an angular velocity of 50°/s.

Pathophysiology of rigidity

Following the assumption of a partial overlap between neuronal loops generating LLRs and brain structures responsible for parkinsonian rigidity, gaining new insights into the pathophysiology of rigidity in PD would require a better understanding of neuronal generators for LLRs. Traditionally, the first line of evidence attributed abnormal LLRs in PD to spinal circuits activated by slowly-conducting group II afferent fibres.^{11,57,58} However, this hypothesis has also been questioned since group II fibres are not sensitive to rapid and short joint displacements, which can elicit LLRs from both proximal and distal muscles of the lower limb, thus suggesting the multifactorial origin of LLRs.^{9,11,36,59} Alternatively, increased LLRs in PD would prominently reflect the abnormal activation of a transcortical neuronal loop involving the activation of the sensorimotor cortex.^{8,52,60,61} This theory would rely on the observation that the latencies of the LLRs for distal hand muscles fit in well with those expected by the transcortical neuronal loop. Also, it has been demonstrated that lesions affecting the transcortical loop could disrupt the LLRs.^{36,61} However, several lines of evidence argue also against this hypothesis since (i) intracranial recordings in an animal model of PD have demonstrated that neuronal activity in the primary motor cortex may be unrelated to the amplitude of stretch-induced LLRs⁶²; (ii) neuroimaging and neurophysiological studies with non-invasive transcranial magnetic stimulation,⁶³ probing the activation of the transcortical sensorimotor loop in PD patients have reported reduced rather than increased cortical activity⁶⁴

after proprioceptive inputs able to elicit LLRs^{36,65–68}, and (iii) a recent study in healthy humans using a plasticity-inducing protocol based on a modified paired associative stimulation^{63,64} demonstrated long-term changes in LLRs as a result of spike timing-dependent plasticity in the reticular formation.⁶⁹ In line with growing experimental data, a more reasonable hypothesis would point to increased LLRs in PD as a result of abnormal activation of the ponto-bulbar reticular formation.^{12,36,62,70–72} Accordingly, the most plausible efferent pathway of the neuronal loop responsible for increased upper limb LLRs in PD would imply hyperactive descending fibres from the ponto-bulbar reticular formation and travelling through the dorsal and medial reticulo-spinal tracts (RSTs). According to this hypothesis, parkinsonian rigidity would result from increased excitability of propriospinal and Ia interneurons through the 'facilitatory' medial RST (which is disinhibited in PD) and in turn leading to the activation of spinal alpha and gamma motor neurons.¹² Also, the concurrent increased activation of the 'inhibitory' dorsal RST would lead to increased inhibition of spinal Ib inhibitory interneurons again contributing to increased activation of spinal alpha motor neurons.^{70,73}

It is more difficult to identify the putative afferent pathways contributing to abnormal LLRs in PD. Possible solutions arise from our new observation of a velocity-dependent feature of increased LLRs in PD. Experimental evidence in animals and humans has demonstrated that the cerebellum would represent the most relevant brain structure gaining LLRs.^{8,36,59,74} Experimental cooling of selective regions of the paleocerebellum induced loss of predictive feedback,

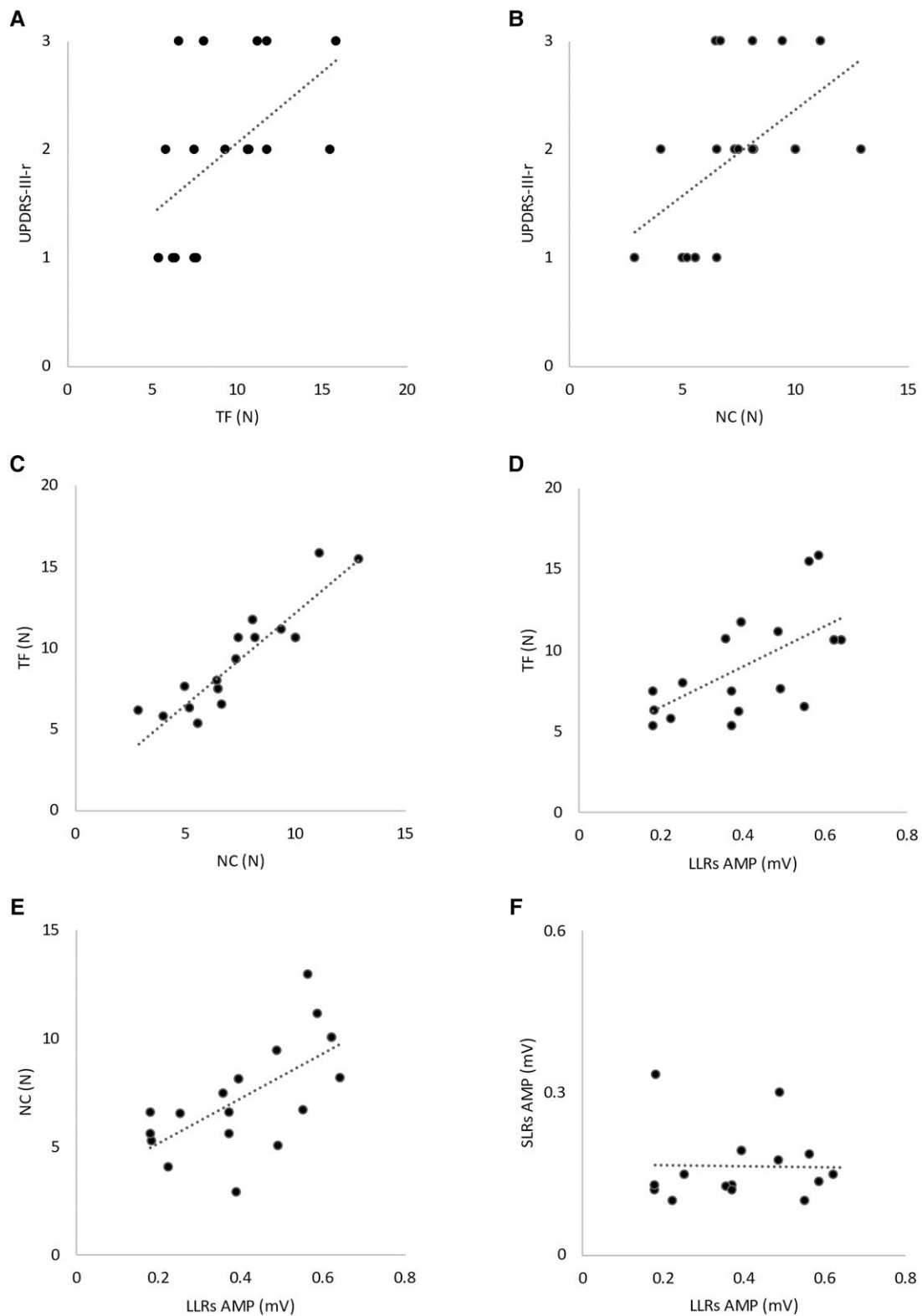


Figure 6 Correlation analysis. Correlation analysis among a specific subset of clinical, biomechanical and neurophysiological measures recorded from Parkinson’s disease (PD) patients during robot-assisted wrist extension (A) Unified Parkinson’s Disease Rating Scale part III (MDS-UPDRS-III-r) versus total force (TF) ($r = 0.61$; $P = 0.004$). (B) MDS-UPDRS-III-r versus neural component (NC) ($r = 0.58$, $P = 0.008$). (C) TF versus NC ($r = 0.86$, $P < 0.01$). (D) TF versus long-latency reflexes (LLRs) amplitudes ($r = 0.57$, $P = 0.01$). (E) NC versus LLRs amplitudes ($r = 0.69$, $P < 0.01$). (F) Short-latency reflexes (SLRs) amplitudes versus LLRs amplitudes ($r = 0.28$, $P = 0.32$). Note that only correlations showed in C and E survived to correction for multiple comparisons, whereas that showed in F was not significant. Also, note that correlations refer to biomechanical and neurophysiological measures collected during robot-assisted wrist extensions delivered at an angular velocity of $280^\circ/s$.

including those responsible for the LLRs.^{75–78} Further supporting the role of the cerebellum, LLRs are typically reduced in patients affected by cerebellar disorders, such as cerebellar ataxia.⁷⁸ Hence, we speculate that the putative neural loop responsible for increased upper limb LLRs in PD would imply the following pathways: stretch-induced activation of Ia and group II afferent fibres→spino-cerebellar pathways→ipsilateral cerebellum→deep cerebellar nuclei→the ponto-bulbar reticular formation through cerebello-reticular connections^{79,80}→medial and dorsal RST→intrinsic spinal cord circuits projecting onto alpha and gamma motor neurons. This hypothetical neuronal loop would also explain the typical LLRs latency resulting from descending slow-conducting non-corticospinal tracts.³⁶ Overall, following the assumption of partial overlap of the neuronal pathways responsible for LLRs and those contributing to parkinsonian rigidity, we speculate that the spino-cerebello-reticulo-spinal pathway here described would be the neuronal underpinning of ‘objective rigidity’ in PD. A final comment concerns how the spino-cerebello-reticulo-spinal pathway putatively responsible for ‘objective rigidity’ in PD can be affected by dopaminergic denervation. Indeed, rigidity is considered a crucial DOPA-responsive parkinsonian feature. Although our study does not clarify the effect of dopaminergic stimulation on biomechanical and neurophysiological measures of ‘objective rigidity’ in PD, a reasonable hypothesis implies that dopaminergic denervation elicits ‘objective rigidity’ in PD through abnormal direct projections to the reticular formation from the basal ganglia⁸¹ or non-primary motor areas, including the supplementary motor areas,^{36,70} or finally indirect connections via the pedunculo-pontine nucleus.^{12,82}

Limitations

First, our findings should not be generalized to the whole population of patients with PD since most of our patients were in the early or mid-stage PD. Hence, we cannot exclude that, in more advanced stages of the disease, parkinsonian rigidity is also associated with changes in intrinsic muscular visco-elastic components. Furthermore, given that our measures have been acquired in patients in the ON state, the present study does not provide any information about the effect of dopaminergic stimulation on biomechanical as well as neurophysiological features of ‘objective rigidity’ in PD. Our observations do not allow us to exclude a cortical origin of LLRs as well as the contribution of the corticospinal tract in combination with the RST in promoting tonic changes in spinal interneuronal excitability. Still, although the present study in early or mid-stage PD showed that ‘objective rigidity’ was associated only with increased LLRs, we do not exclude that, in more advanced stages of the disease, besides LLRs, additional phasic or tonic reflexes would contribute to parkinsonian rigidity. Lastly, when evaluating our clinico-neurophysiological correlations, it should be considered that in addition to stretch-induced EMG responses, parkinsonian rigidity would also result from patient inability to voluntarily relax. Such a component was eliminated with our method since we did not include trials with background EMG activity.

Conclusions

The present study provides experimental evidence showing that LLRs contribute to the neural component of ‘objective rigidity’ in PD. Also, the velocity-dependent feature of ‘objective rigidity’ in PD helped us to speculate about the putative neuronal pathway responsible for this relevant parkinsonian sign. We recognize that this is an exploratory study and future investigations in the field

also using other instrumental devices are required to clarify the role of our putative neuronal pathway in the pathophysiology of rigidity in PD. Lastly, concerning the effect of L-DOPA, we expect that patients with PD ON therapy would manifest lower ‘objective rigidity’ and smaller LLRs than patients OFF treatment. However, future studies will clarify the impact of L-DOPA on biomechanical and neurophysiological measures of ‘objective rigidity’ and whether the underlying pathophysiological mechanisms maintain the same relationship with each other in patients with PD OFF as ON therapy.

Acknowledgements

M.H. is supported by the NINDS Intramural Program.

Funding

No funding was received towards this work.

Competing interests

The authors report no competing interests.

Supplementary material

Supplementary material is available at *Brain* online.

References

1. Postuma RB, Berg D, Stern M, et al. MDS Clinical diagnostic criteria for Parkinson’s disease. *Mov Disord*. 2015;30:1591–1601.
2. Obeso JA, Stamelou M, Goetz CG, et al. Past, present, and future of Parkinson’s disease: a special essay on the 200th anniversary of the shaking palsy. *Mov Disord*. 2017;32:1264–1310.
3. Broussolle E, Krack P, Thobois S, Xie-Brustolin J, Pollak P, Goetz CG. Contribution of Jules Froment to the study of parkinsonian rigidity. *Mov Disord*. 2007;22:909–914.
4. Fung T, Fung VS, Thompson PD. Rigidity & spasticity. In: Jankovic JJ, Tolosa E, eds. *Parkinson’s disease and movement disorders*. 4th ed. Lippencott Williams & Wilkens; 2002:473–482
5. Antonini A, Abbruzzese G, Ferini-Strambi L, et al. Validation of the Italian version of the movement disorder society–unified Parkinson’s disease rating scale. *Neurol Sci*. 2013;34:683–687.
6. Rizzo G, Copetti M, Arcuti S, Martino D, Fontana A, Logroscino G. Accuracy of clinical diagnosis of Parkinson disease: a systematic review and meta-analysis. *Neurology*. 2016;86:566–576.
7. Hagbarth KE, Hägglund JV, Wallin EU, Young RR. Grouped spindle and electromyographic responses to abrupt wrist extension movements in man. *J Physiol*. 1981;312:81–96.
8. Kurtzer I, Pruszynski JA, Scott SH. Long-latency and voluntary responses to an arm displacement can be rapidly attenuated by perturbation offset. *J Neurophysiol*. 2010;103:3195–3204.
9. Lewis GN, Perreault EJ, MacKinnon CD. The influence of perturbation duration and velocity on the long-latency response to stretch in the biceps muscle. *Exp Brain Res*. 2005;163:361–369.
10. Schuurmans J, de Vlught E, Schouten AC, Meskers CGM, de Groot JH, van der Helm FCT. The monosynaptic Ia afferent pathway can largely explain the stretch duration effect of the long latency M2 response. *Exp Brain Res*. 2009;193:491–500.
11. Berardelli A, Sabra AF, Hallett M. Physiological mechanisms of rigidity in Parkinson’s disease. *J Neurol Neurosurg Psychiatry*. 1983;46:45–53.

12. Delwaide PJ. Parkinsonian rigidity. *Funct Neurol*. 2001;16:147-156.
13. Meara RJ, Cody FWJ. Relationship between electromyographic activity and clinically assessed rigidity studied at the wrist joint in Parkinson's disease. *Brain*. 1992;115(Pt 4):1167-1180.
14. Rothwell JC, Obeso JA, Traub MM, Marsden CD. The behaviour of the long-latency stretch reflex in patients with Parkinson's disease. *J Neurol Neurosurg Psychiatry*. 1983;46:35-44.
15. Tatton WG, Bedingham W, Verrier MC, Blair RD. Characteristic alterations in responses to imposed wrist displacements in parkinsonian rigidity and dystonia musculorum deformans. *Can J Neurol Sci*. 1984;11:281-287.
16. Cody FWJ, Macdermott N, Matthews PBC, Richardson HC. Observations on the genesis of the stretch reflex in Parkinson's disease. *Brain*. 1986;109(Pt 2):229-249.
17. Perera T, Lee WL, Jones M, et al. A palm-worn device to quantify rigidity in Parkinson's disease. *J Neurosci Methods*. 2019;317:113-120.
18. Bloem BR, Okun MS, Klein C. Parkinson's disease. *Lancet*. 2021;397:2284-2303.
19. Wichmann T, DeLong MR, Guridi J, Obeso JA. Milestones in research on the pathophysiology of Parkinson's disease. *Mov Disord*. 2011;26:1032-1041.
20. Marusiak J, Jaskólska A, Budrewicz S, Koszewicz M, Jaskólski A. Increased muscle belly and tendon stiffness in patients with Parkinson's disease, as measured by myotonometry. *Mov Disord*. 2011;26:2119-2122.
21. Xia R, Muthumani A, Mao ZH, Powell DW. Quantification of neural reflex and muscular intrinsic contributions to parkinsonian rigidity. *Exp Brain Res*. 2016;234:3587-3595.
22. Zetterberg H, Frykberg GE, Gäverth J, Lindberg PG. Neural and nonneural contributions to wrist rigidity in Parkinson's disease: an explorative study using the NeuroFlexor. *BioMed Res Int*. 2015;2015:276182.
23. Xia R, Rymer WZ. The role of shortening reaction in mediating rigidity in Parkinson's disease. *Exp Brain Res*. 2004;156:524-528.
24. Oldfield RC. The assessment and analysis of handedness: The Edinburgh inventory. *Neuropsychologia*. 1971;9:97-113.
25. Bhidayasiri R, Tarsy D. Parkinson's disease: Hoehn and Yahr scale. In: Bhidayasiri R, Tarsy D, eds. *Movement disorders: A video atlas*. Humana Press; 2012:4-5.
26. Dalrymple-Alford JC, MacAskill MR, Nakas CT, et al. The MoCA: Well-suited screen for cognitive impairment in Parkinson disease. *Neurology*. 2010;75:1717-1725.
27. Dubois B, Slachevsky A, Litvan I, Pillon B. The FAB: A frontal assessment battery at bedside. *Neurology*. 2000;55:1621-1626.
28. Hamilton M. A rating scale for depression. *J Neurol Neurosurg Psychiatry*. 1960;23:56-62.
29. Jahanshahi M, Jones CRG, Zijlmans J, et al. Dopaminergic modulation of striato-frontal connectivity during motor timing in Parkinson's disease. *Brain*. 2010;133(Pt 3):727-745.
30. Pennati GV, Plantin J, Borg J, Lindberg PG. Normative NeuroFlexor data for detection of spasticity after stroke: a cross-sectional study. *J Neuroeng Rehabil*. 2016;13:30.
31. Lindberg PG, Gäverth J, Islam M, Fagergren A, Borg J, Forssberg H. Validation of a new biomechanical model to measure muscle tone in spastic muscles. *Neurorehabil Neural Repair*. 2011;25:617-625.
32. Gäverth J, Eliasson AC, Kullander K, Borg J, Lindberg PG, Forssberg H. Sensitivity of the NeuroFlexor method to measure change in spasticity after treatment with botulinum toxin A in wrist and finger muscles. *J Rehabil Med*. 2014;46:629-634.
33. Andringa A, Meskers C, van de Port I, et al. Quantifying neural and non-neural components of wrist hyper-resistance after stroke: comparing two instrumented assessment methods. *Med Eng Phys*. 2021;98:57-64.
34. Wang R, Herman P, Ekeberg Ö, Gäverth J, Fagergren A, Forssberg H. Neural and non-neural related properties in the spastic wrist flexors: an optimization study. *Med Eng Phys*. 2017;47:198-209.
35. Gäverth J, Sandgren M, Lindberg PG, Forssberg H, Eliasson AC. Test-retest and inter-rater reliability of a method to measure wrist and finger spasticity. *J Rehabil Med*. 2013;45:630-636.
36. Kurtzer IL. Long-latency reflexes account for limb biomechanics through several supraspinal pathways. *Front Integr Neurosci*. 2015;8:99.
37. Ferreira-Sánchez MDR, Moreno-Verdú M, Cano-de-la-Cuerda R. Quantitative measurement of rigidity in Parkinson's disease: a systematic review. *Sensors*. 2020;20:880.
38. Proske U, Wise AK, Gregory JE. The role of muscle receptors in the detection of movements. *Prog Neurobiol*. 2000;60:85-96.
39. Teräväinen H, Tsui JKC, Mak E, Calne DB. Optimal indices for testing parkinsonian rigidity. *Can J Neurol Sci*. 1989;16:180-183.
40. Halaki M, O'Dwyer N, Cathers I. Systematic nonlinear relations between displacement amplitude and joint mechanics at the human wrist. *J Biomech*. 2006;39:2171-2182.
41. Koo TTK, Mak AFT. A neuromusculoskeletal model to simulate the constant angular velocity elbow extension test of spasticity. *Med Eng Phys*. 2006;28:60-69.
42. Perotto AO. *Anatomical guide for the electromyographer*. 3rd Ed. Charles Thomas; 1994.
43. Kurtzer IL, Pruszynski JA, Scott SH. Long-latency reflexes of the human arm reflect an internal model of limb dynamics. *Curr Biol*. 2008;18:449-453.
44. Tatton WG, Lee RG. Evidence for abnormal long-loop reflexes in rigid Parkinsonian patients. *Brain Res*. 1975;100:671-676.
45. Albers C. The problem with unadjusted multiple and sequential statistical testing. *Nat Commun*. 2019;10:1921.
46. Shuster JJ, Neu J. A pocock approach to sequential meta-analysis of clinical trials: Pocock sequential meta-analysis. *Res Synth Methods*. 2013;4:269-279.
47. Armitage P, McPherson CK, Rowe BC. Repeated significance tests on accumulating data. *J R Stat Soc Ser Gen*. 1969;132:235.
48. Lee HM, Huang YZ, Chen JJJ, Hwang IS. Quantitative analysis of the velocity related pathophysiology of spasticity and rigidity in the elbow flexors. *J Neurol Neurosurg Psychiatry*. 2002;72:621-629.
49. Mak MKY, Wong ECY, Hui-Chan CWY. Quantitative measurement of trunk rigidity in parkinsonian patients. *J Neurol*. 2007;254:202-209.
50. Powell D, Threlkeld AJ, Fang X, Muthumani A, Xia R. Amplitude- and velocity-dependency of rigidity measured at the wrist in Parkinson's disease. *Clin Neurophysiol*. 2012;123:764-773.
51. Xia R, Sun J, Threlkeld AJ. Analysis of interactive effect of stretch reflex and shortening reaction on rigidity in Parkinson's disease. *Clin Neurophysiol*. 2009;120:1400-1407.
52. Chen R, Berardelli A, Bhattacharya A, et al. Clinical neurophysiology of Parkinson's disease and parkinsonism. *Clin Neurophysiol Pract*. 2022;7:201-227.
53. Bergui M, Lopiano L, Paglia G, Quattrocchio G, Scarzella L, Bergamasco B. Stretch reflex of quadriceps femoris and its relation to rigidity in Parkinson's disease. *Acta Neurol Scand*. 1992;86:226-229.
54. Trompetto C, Marinelli L, Mori L, et al. Pathophysiology of spasticity: implications for neurorehabilitation. *BioMed Res Int*. 2014;2014:354906.
55. Miscio G, Pisano F, Del Conte C, Pianca D, Colombo R, Schieppati M. The shortening reaction of forearm muscles: the influence of central set. *Clin Neurophysiol*. 2001;112:884-894.

56. Xia R, Powell D, Rymer WZ, Hanson N, Fang X, Threlkeld AJ. Differentiation between the contributions of shortening reaction and stretch-induced inhibition to rigidity in Parkinson's disease. *Exp Brain Res*. 2011;209:609-618.
57. Lourenço G, Iglesias C, Cavallari P, Pierrot-Deseilligny E, Marchand-Pauvert V. Mediation of late excitation from human hand muscles via parallel group II spinal and group I transcortical pathways. *J Physiol*. 2006;572(Pt 2):585-603.
58. Meskers CGM, Schouten AC, Rich MML, de Groot JH, Schuurmans J, Arendzen JH. Tizanidine does not affect the linear relation of stretch duration to the long latency M2 response of m. flexor carpi radialis. *Exp Brain Res*. 2010;201:681-688.
59. Pruszynski JA, Scott SH. Optimal feedback control and the long-latency stretch response. *Exp Brain Res*. 2012;218:341-359.
60. MacKinnon CD, Verrier MC, Tatton WG. Motor cortical potentials precede long-latency EMG activity evoked by imposed displacements of the human wrist. *Exp Brain Res*. 2000;131:477-490.
61. Pruszynski JA, Kurtzer I, Nashed JY, Omrani M, Brouwer B, Scott SH. Primary motor cortex underlies multi-joint integration for fast feedback control. *Nature*. 2011; 478:387-390.
62. Pasquereau B, Turner RS. Primary motor cortex of the parkinsonian monkey: altered neuronal responses to muscle stretch. *Front Syst Neurosci*. 2013;7:98.
63. Suppa A, Ascì F, Guerra A. Transcranial magnetic stimulation as a tool to induce and explore plasticity in humans. *Handb Clin Neurol*. 2022;184:73-89.
64. Suppa A, Quartarone A, Siebner H, et al. The associative brain at work: evidence from paired associative stimulation studies in humans. *Clin Neurophysiol*. 2017;128:2140-2164.
65. Boecker H, Ceballos-Baumann A, Bartenstein P, et al. Sensory processing in Parkinson's and Huntington's disease: investigations with 3D H(2)(15)O-PET. *Brain J Neurol*. 1999;122(Pt 9): 1651-1665.
66. DeLong MR, Wichmann T. Circuits and circuit disorders of the basal ganglia. *Arch Neurol*. 2007;64:20-24.
67. Lewis GN, Byblow WD. Altered sensorimotor integration in Parkinson's disease. *Brain*. 2002;125(Pt 9):2089-2099.
68. Rossini PM, Babiloni F, Bernardi G, et al. Abnormalities of short-latency somatosensory evoked potentials in parkinsonian patients. *Electroencephalogr Clin Neurophysiol*. 1989;74:277-289.
69. Foysal KMR, de Carvalho F, Baker SN. Spike timing-dependent plasticity in the long-latency stretch reflex following paired stimulation from a wearable electronic device. *J Neurosci*. 2016; 36:10823-10830.
70. Ganguly J, Kulshreshtha D, Almotiri M, Jog M. Muscle tone physiology and abnormalities. *Toxins (Basel)*. 2021;13:282.
71. Marchand-Pauvert V, Gerdelat-Mas A, Ory-Magne F, et al. Both L-DOPA and HFS-STN restore the enhanced group II spinal reflex excitation to a normal level in patients with Parkinson's disease. *Clin Neurophysiol*. 2011;122:1019-1026.
72. Ravichandran VJ, Honeycutt CF, Shemmell J, Perreault EJ. Instruction-dependent modulation of the long-latency stretch reflex is associated with indicators of startle. *Exp Brain Res*. 2013;230:59-69.
73. Delwaide PJ, Pepin JL, de Noordhout A M. Short-latency autogenic inhibition in patients with parkinsonian rigidity. *Ann Neurol*. 1991;30:83-89.
74. Ebner TJ, Hewitt AL, Popa LS. What features of limb movements are encoded in the discharge of cerebellar neurons? *Cerebellum*. 2011;10:683-693.
75. Friedemann HH, Noth J, Diener HC, Bacher M. Long latency EMG responses in hand and leg muscles: Cerebellar disorders. *J Neurol Neurosurg Psychiatry*. 1987;50:71-77.
76. Hore J, Flament D. Evidence that a disordered servo-like mechanism contributes to tremor in movements during cerebellar dysfunction. *J Neurophysiol*. 1986;56:123-136.
77. Hore J, Vilis T. Loss of set in muscle responses to limb perturbations during cerebellar dysfunction. *J Neurophysiol*. 1984;51: 1137-1148.
78. Kurtzer I, Trautman P, Rasquinha RJ, Bhanpuri NH, Scott SH, Bastian AJ. Cerebellar damage diminishes long-latency responses to multijoint perturbations. *J Neurophysiol*. 2013;109: 2228-2241.
79. Hammar I, Krutki P, Drzymala-Celichowska H, Nilsson E, Jankowska E. A trans-spinal loop between neurones in the reticular formation and in the cerebellum. *J Physiol*. 2011;589(Pt 3):653-665.
80. Therrien AS, Bastian AJ. The cerebellum as a movement sensor. *Neurosci Lett*. 2019;688:37-40.
81. Chronister RB, Walding JS, Aldes LD, Marco LA. Interconnections between substantia nigra reticulata and medullary reticular formation. *Brain Res Bull*. 1988;21:313-317.
82. Bostan AC, Dum RP, Strick PL. The basal ganglia communicate with the cerebellum. *Proc Natl Acad Sci U S A*. 2010;107:8452-8456.